〈논 문〉 SAE NO. 953704

Analysis of the Initial Combustion Period for the Ultra Lean Burn Engine

초희박연소기관을 위한 초기연소구간의 해석

S. B. Han,* N. H. Lee,** S. Y. Lee***
한 성 빈, 이 내 현, 이 성 열

ABSTRACT

스파크 점화기관에서 화염전파과정에 관한 연구를 수행하기 위하여는, 초기화염핵 구간에서의 화염의 형성과 발달의 거동을 정확히 파악하여야 한다.

그러므로 화염핵의 형성과 발달에 영향을 미치는 최소 화염핵 크기의 이론적인 계산을 수행하였다. 이론식을 정립하기 위하여 열점화 이론을 이용하였다.

최소 화염핵 크기를 계산하기 위해 열전도 계수, 화염온도, 층류연소속도, 기타 열역학적 상태량 등을 계산하였다.

계산에 의존한 화염핵 크기의 신뢰성을 확인하기 위하여, 점화에너지를 변화시킬 수 있는 점화장치를 사용하여 실기 운전을 통하여 희박연소 한계가 그 때의 화염핵이 성정할 수 있는 영역이라고 가정하여 그 정확도를 확인 하였다.

주요기술용어 : Thermal Ignition Theory(열점화 이론), Thermal Conductivity(열전도 계수), Flame Kernel Radius(화염핵 반경), Lean Misfirnig Limit(희박 연소 영역)

Nomenclature

a	: excess fuel	l	: mean free path
B	: Boltzmann constant	N	: molecule per unit volume
C_p	: specific heat at constant pressure	N_A	: Avogadro's number
C_v	: specific heat at constant volume	P	: pressure
C_{vm}	: molecular heat capacity	q	: heating value
ΔH_F	: enthalpy difference of products	Q_c	: heat release at adiabatic process
K_1, K_2	: equilibrium constant	Q_F	: heat release in 1 kmol mixture
		R	: universal gas constant
		R_F	: flame kernel radius

* 정회원, 인덕전문대학 기계과
** 정회원, 기아기술센터 엔진연구실
*** 정회원, 성균관대학교 기계공학과

R_{min} : minimum flame kernel radius
V_L : laminar burning velocity
T : temperature
u : internal energy
V : volume
V_o : mole volume
V_m : mean molecular velocity
X : mole fraction of fuel
Y : mole fraction
$\propto$: thermal conductivity
σ : collision cross section
ρ : density
R : gas constant

〈Subscripts〉

m : mean
o, u : unburned
f, F : flame, mixture
i : i th component
1 : initial

1. Introduction

Combustion fluctuation of a spark ignition engine influences the emission of HC, CO and others as well as increasing fuel consumption. Ignition enhancement in conjunction with lean combustion concepts are very promising approaches for better fuel consumption and lower emission. A major defect in applying these concepts is the increasing cyclic fluctuation or variability in the pressure curve for leaner mixtures. This is caused by the variation of chemical and physical conditions at spark timing and the hindered flame propagetion by the flame early in the combustion process at leaner air-fuel ratios. Therefore, a short initial combustion period is most important for the development of the whole combustion period.[1-3]

It is recognized that cyclic variations in combustion of spark ignition engine originate during the initial stage of combustion from the time of the spark breakdown to the early flame phase. That is, the initial stage of combustion governs overall combustion in a spark ignition engine. This initial stage can be stablized by creating a large flame that is obtained through improvements of the spark discharge process in the conventional ignition system, i.e., the spark discharge goes to breakdown mode that is far better suited for inflamming the combustible mixture than arc or glow discharge. It is, however, difficult to find report on the theory of formation of spark and flame kernel by breakdown mode. Thus, it is not clear why the breakdown is superior to the others. Accordingly, it is imporssible to find out a better method for improving the spark discharge process.[4-5]

To decrease combustion fluctuation in lean mixtures, a stablized flame kernel must be formed in a short time so that the period of initial flame growth is shortened.[6]

The approach taken in this research to deal with the lean combustion problems, is to increase combustion efficiency by using a better ignition system. This increases the flame kernel size and reduce the ignition delay and combustion duration. It is well known that fast burning decreases cyclic variation, extends the lean misfire limit, and improves fuel economy.

The dependence of the overall combustion on the early burn period was also recognized by researchers.[7] From high speed movies of combustion in an engine, it was noted that the fully devoloped flame travel phase is the most repeatable combustion stage. The period from spark to the establishment of a fully develped flame and the post-flame combustion stage were most variable from cycle to cycle. If the variations of the early combustion period could be reduced, the variations in the later stage would also diminish.[8]

Therefore, to accomplish these ends, the causes of the combustion variation, as well as the effects of air-fuel ratio, flame kernel size, and the ignition energy, must be fully understood.

To study flame propagation in a spark ignition engine, it must concentrate on initial combustion stage when the flame is formed and developed.[9-11)]

In this paper, the size of the flame kernel was calculated theoretically. And it was analysed theoretically the theory of development process of flame kernel to predict a best way for creating a large flame kernel in a spark ignition engine.

2. Theoretical Background of Flame Kernel Radius

To form the stable flame kernel, it can be based on the thermal ignition model. The flame kernel is formed by oxidation reaction from the surface of spark kernel. If the heat capacity produced in the reaction zone is greater than the heat loss in the reaction surface, the flame develop.

The mimimum flame kernel radius is the smallest radius of flame kernel that must be developed flame kernel. To contribute to the heat flux across the front by diffusion and heat conduction are summarized into a single transport coefficient, α, with the dimension of heat conductivity. Assuming spherical geometry and constant pressure, we obtain by a linearization of the problem, the following expressions for the energy differences in an unreacted volume element ΔV during the time interval Δt(see Figure 1). Available energy ΔQ^V in ΔV is calculated as follows :

$$\Delta Q^V = \frac{(Xq - \Delta H_F)}{V_o} 4\pi\ r^2\ \Delta r$$

$$= \frac{(Xq - \Delta H_F)P_o}{R\ T_o} 4\pi\ r^2\ \Delta r, \qquad (1)$$

where X_q=molar heat of combustion, ΔH_F=molar enthalpy required to heat the reaction products to flame temperature, and V_o=molar volume. Net energy loss over the cold surface is calculated as follows :

$$\Delta Q_A = \alpha \frac{(T_F - T_o)}{\Delta r}\quad \Delta t\ 8\pi\ r\ \Delta r. \qquad (2)$$

A self-sustained flame propagation occurs only if the net surface loss never exceeds the available energy in the volume element ; thus

$$\Delta Q^V / \Delta Q^A \geq 1, \qquad (3)$$

or clearly

$$\frac{(Xq - \Delta H_F)P_o}{R\ T_o} 4\pi\ r^2\ \Delta r >$$

$$\alpha \frac{(T_F - T_o)}{\Delta r}\quad \Delta t\ 8\pi\ r\ \Delta r. \qquad (4)$$

Propagation conditions are the more favorable the larger the distance of the front from the discharge center. Prior to self-sustained propagation $\Delta r/\Delta t = V_L$ where V_L is the laminar burning velocity. Therefore, one calculates a minimum radius of the flame kernel required for successful inflammation :

$$R_{min} = \frac{2R\ \alpha\ T_o(T_F - T_o)}{P_o(Xq - \Delta H_F)V_L} \qquad (5)$$

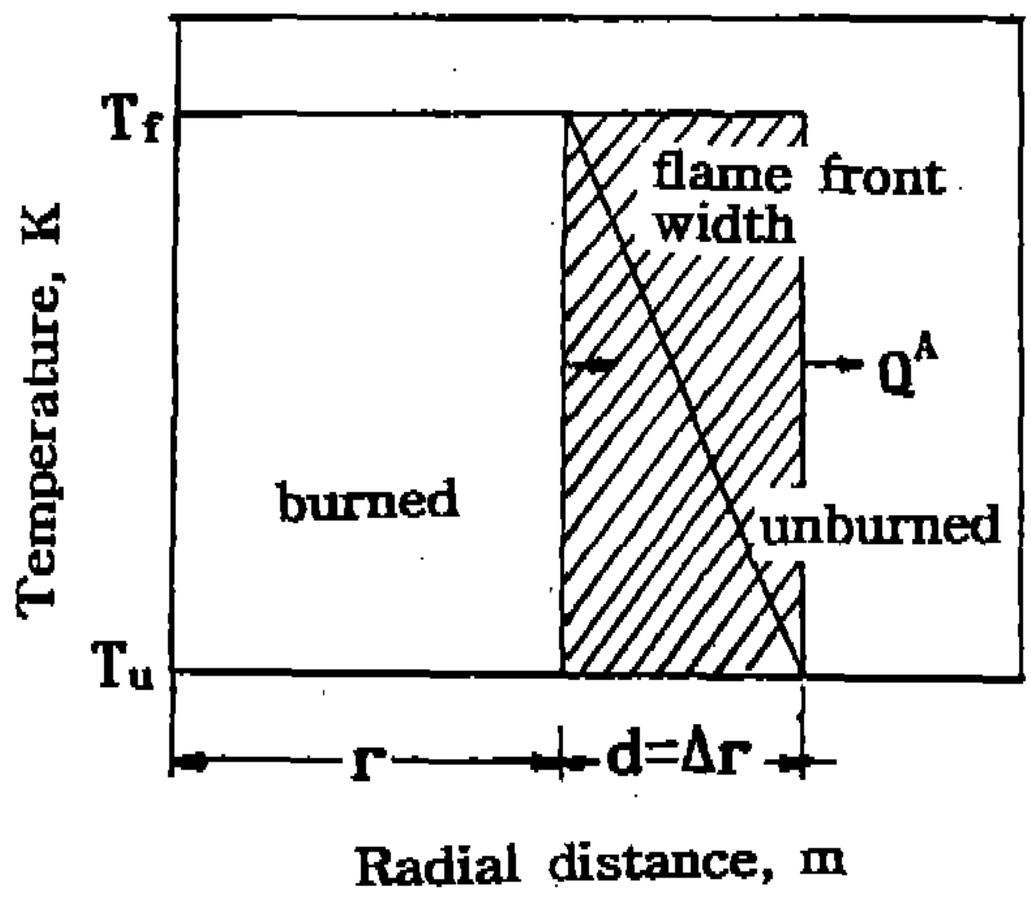

Fig.1 Simplified flame kernel model

Here, to calculate the minimum flame kernel radius, we must know the thermal conductivity, flame temperature, laminar burning velocity, thermodynamic properties, etc.

It is not necessary to consider the heat convection and radiation in the flame front area. Therefore, to determinate thermal conductivity $\propto$, we may consider the heat transfer by molecular kinetic, and determine thermal conductivity of molecular kinetic theory.[12] The thermal conductivity, $\propto$, is represented by the fundamental molecular kinetic theory as follows :

$$\alpha=\frac{1}{3} N V_m C_{vm} l, \quad (6)$$

where the mean molecular velocity, V_m, is

$$V_m=\sqrt{\frac{8BT_o}{\pi\sum(YiMi)}} \quad (7)$$

If the molecules have the Maxwell velocity distribution, the mean free path becomes

$$l=\frac{0.707}{N\sum(Y_i \sigma_i)} \quad (8)$$

The collisional cross-section, σ, of a single molecule is the area of a circle of radius D, the exclusion radius :

$$\sigma_i=\pi D_i^2 \quad (9)$$

Therefore, the thermal conductivity $\propto$ is represented from the EQ (6) to (9) as follow :

$$\alpha=\frac{0.707 C_v}{3N_A \sum(Y_i M_i)} \sqrt{\frac{8BT_o}{\pi\sum(YiMi)}} \quad (10)$$

3. Experimental Apparatus and Procedures

Figure 2 shows the schematic diagram of the engine tested. The engine which was spark ignited had a compression ratio of 7.0, 4-cylinders, and a displacement of 1600cc.

The performance was tested by connecting the crank shaft to the dynamometer. Water brake dynamometer (110kw) was directly connected to the crank shaft of the engine. To measure the volume of the intake air, the orifice flow meter(round type, 25mm) was installed to the intake pipe. This surge tank which was larger than the displacement volume was also installed to decrease the fluctuation of the intake air. Fuel was supplied to the engine by gravity. Carburetor was installed inside the surge tank to provide an equivalent temperature condition. Fuel consumption was measured by the digital fuel consumption meter per 100cc.

The spark advance also was fixed to MBT (mi-

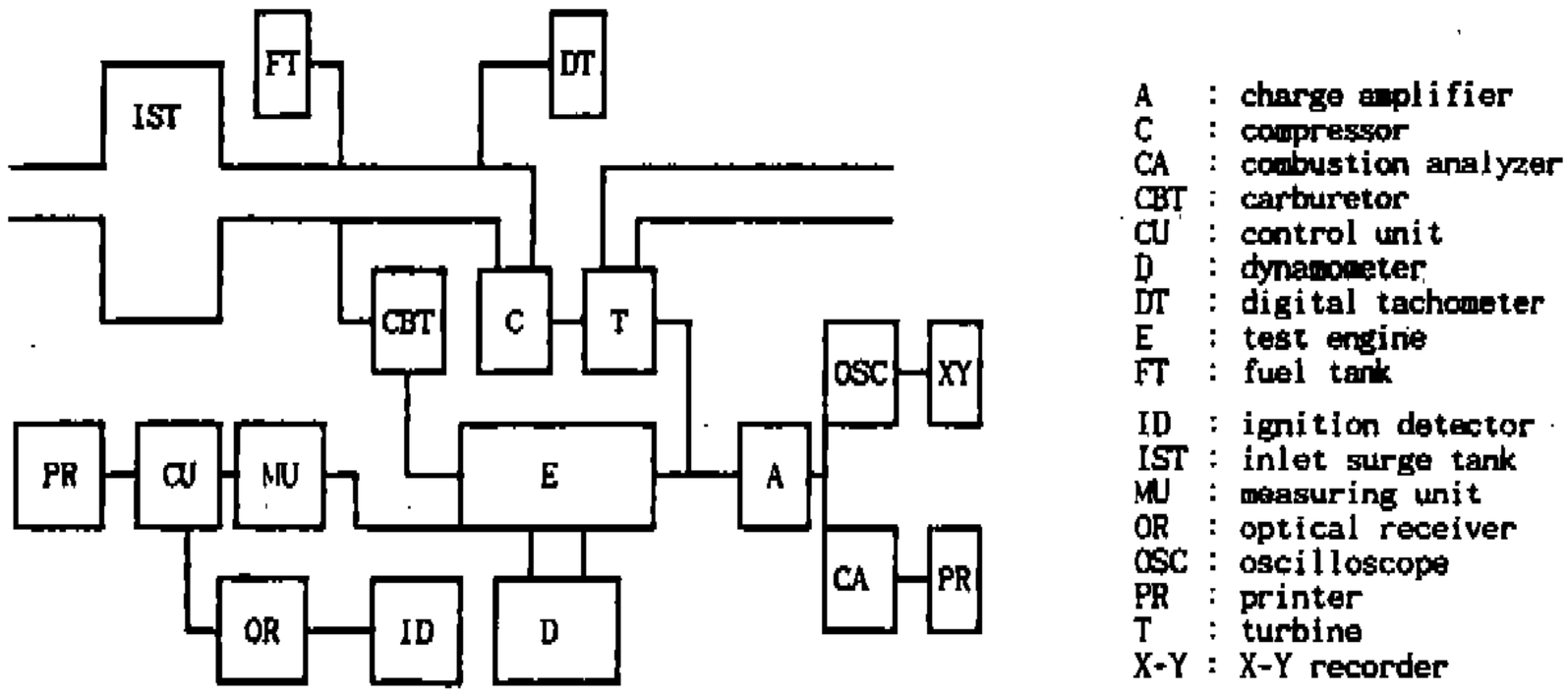

Fig.2 Schematic diagram of experimental apparatus

nimum spark advance for best torque), and the air-fuel ratios were varied. The spark timing was adjusted by changing the angle of the breaker. The engine speed was fixed to 2000rpm which produced the maximum torque.

An ionization probe was fabricated to measure the turbulent flame velocity and was inserted into the cylinder head as shown Fig.3. The ionization probe was located on the cylinder head, 47mm apart from the spark plug, and measured the time of the ionized flame travelled. To obtain the turbulent flame velocity, the time travelled was divided by the travel distance (47mm). The turbulent flame velocities were measured durning the test. The flame propagation velocities were obtained by dividing the distance between the spark plug and the ionization probes by the arrival time of the flame front. The ionization probes used for this test run were those of the spark plugs of motor bicycle and had the 0.8mm gap. To avoid the cyclic numbers counted were up to two hundred cycles and were adjusted by the control unit.

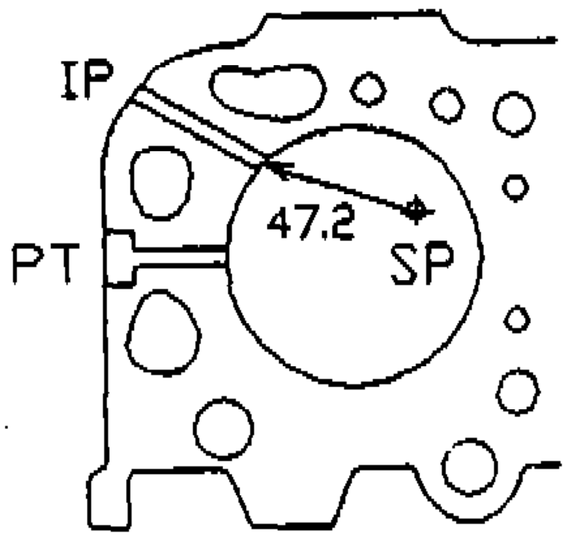

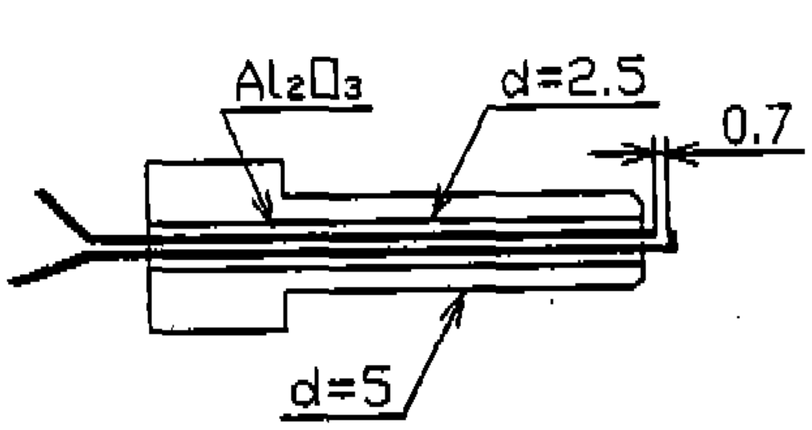

Fig.3 Inserted location of ionization probe and pressure transducer

4. Size of the minimum flame kernel

4.1 Determination of Various Factors

Figure 4 shows the result of the thermal conductivity versus air fuel ratio. In Figure 5, flame temperature T_F versus air fuel ratio is shown by theoretical calculation accounting of the thermal dissociation.

To find the minimum flame kernel radius by the EQ(5) a number of unknown parameters should be estimated. The laminar burning velocity, V_L, in the EQ(5) had been proposed by Van Tiggelen and Deckers[13], Richard and Melven[14], and Kuehl, et al.[15]. But each of the laminar burning velocities proposed have different forms. It was

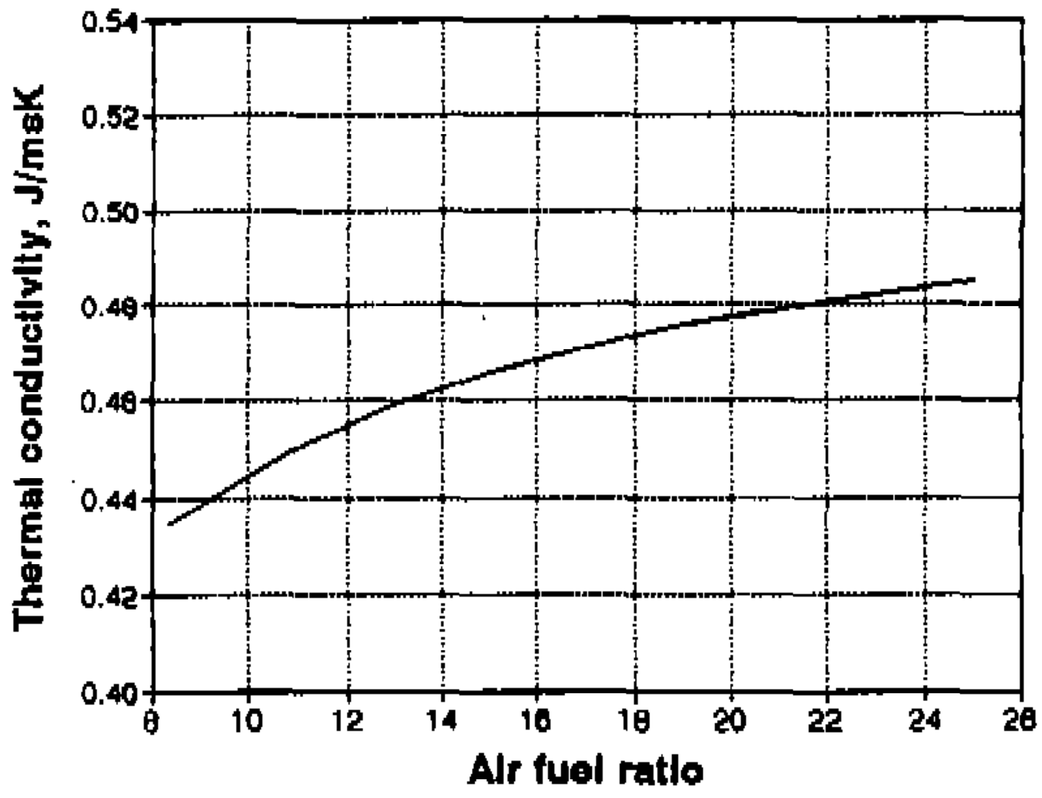

Fig.4 Thermal conductivity with air fuel ratio

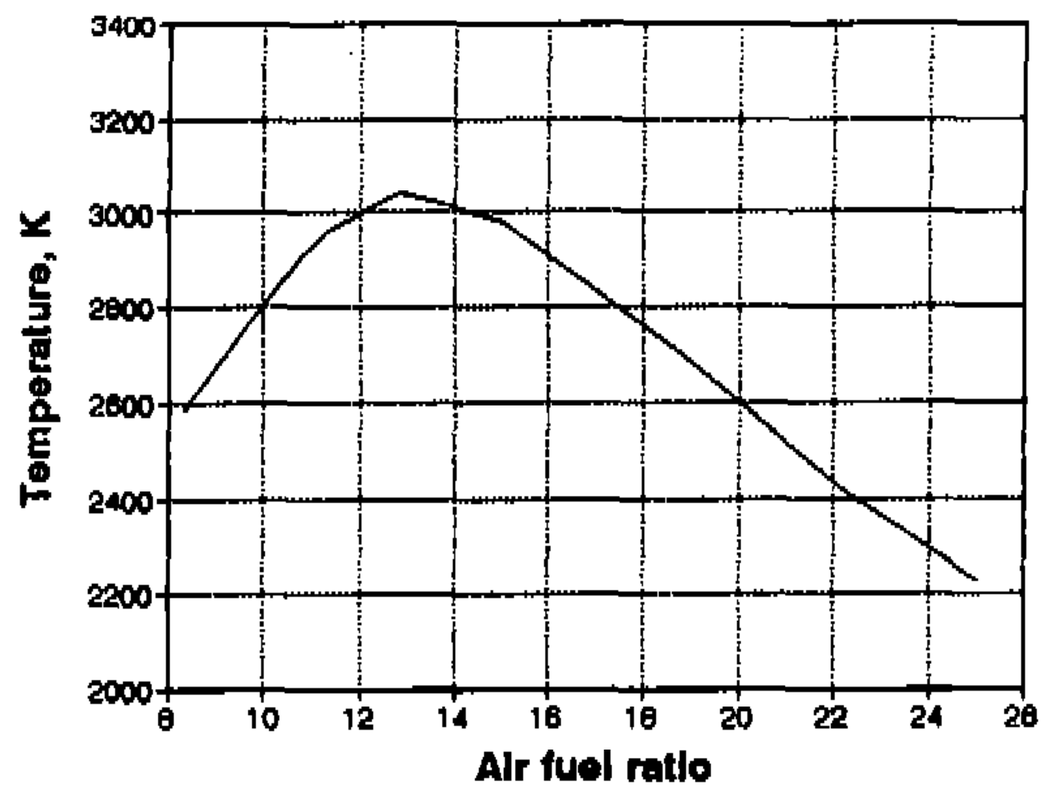

Fig.5 Flame temperature with air fuel ratio

preferred to select the appropriate equation for the laminar burning velocity prior to calculate the velocity.

Figure 6 shows the laminar burning velocities calculated versus the variation in air fuel ratio. From the air fuel ratio 8 : 1 to 25 : 1, the laminar burning velocities were calculated. The equations proposed by Van Tiggelen, Deckers, Richard, Melvin and Kuehl were used to calculate the laminar burning velocities.

To find out the appropriate equation among the equations of the laminar burning velocities, the turbulent flame velocities were measured experimentally. Also, the diagram of the turbulent flame velocity was qualitively compared to that of the laminar burning velocity based on the equations proposed. Among the diagrams from the laminar burning velocities, the best fit to the diagram of the turbulent flame velocity was chosen to be the appropriate laminar burning velocity diagram.

Figure 7 shows the test results of the turbulent flame velocity taking the variation in air fuel ratio into consideration. The maximum turbulent flame velocity was achieved around the air fuel ratio 13 : 1. Based on the above test results of the turbulent flame velocity, the appropriate equation for the laminar burning velocity was selected.

By comparing Fig.6 and Fig.7, the laminar burning velocities based on the Van Tiggelen and Decker's equations were not consistent with the turbulent flame velocity. However, the laminar burning velocities based on the equations of Richard and Melvin, and Kuehl et al. were qualitively consistent with those measurements and found to be acceptable.

Some of the other test results were compared to decide the acceptability of the laminar burning velocities equations based on the methods of Richard and Melvin and Kuehl, et al. The test result with methanol, which was done by Hirano[16], showed : that the laminar burning velocity increased linearly according to the temperature increase of the air fuel mixture. The maximum laminar burning velocity 2.5m/s appeared at the unburned mixture temperature 713K.

The test result of the propane doen by Kuehl showed : that the maximum laminar burning velocity of 2.6m/s appeared at the unburned mixture temperature 811K and at the pressure 30inHg.

This paper calculated the laminar burning velocity of the iso-octane at the initial temperature of 700K the pressure of 400inHg.

It was assumed that the maximum laminar burning velocity of 2.5m/s appeared at the unburned mixture temperature of 700K and at the pressure of 40inHg. However, the calculation results based

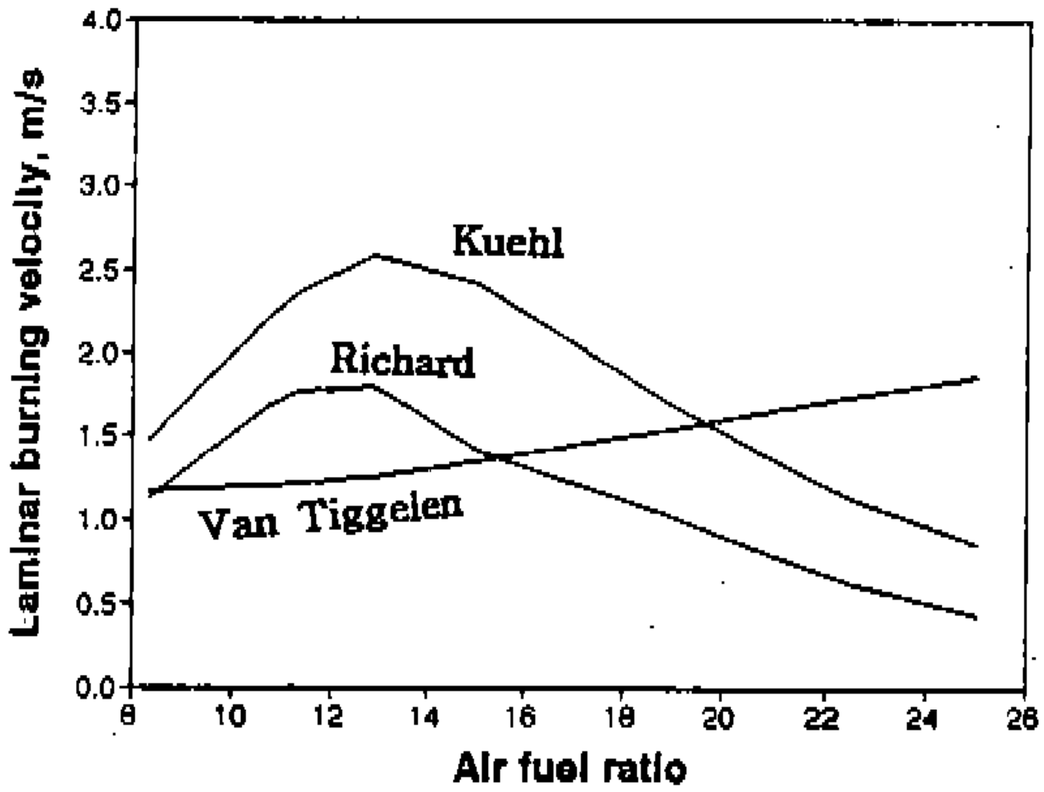

Fig.6 Laminar burning velocity with air fuel ratio

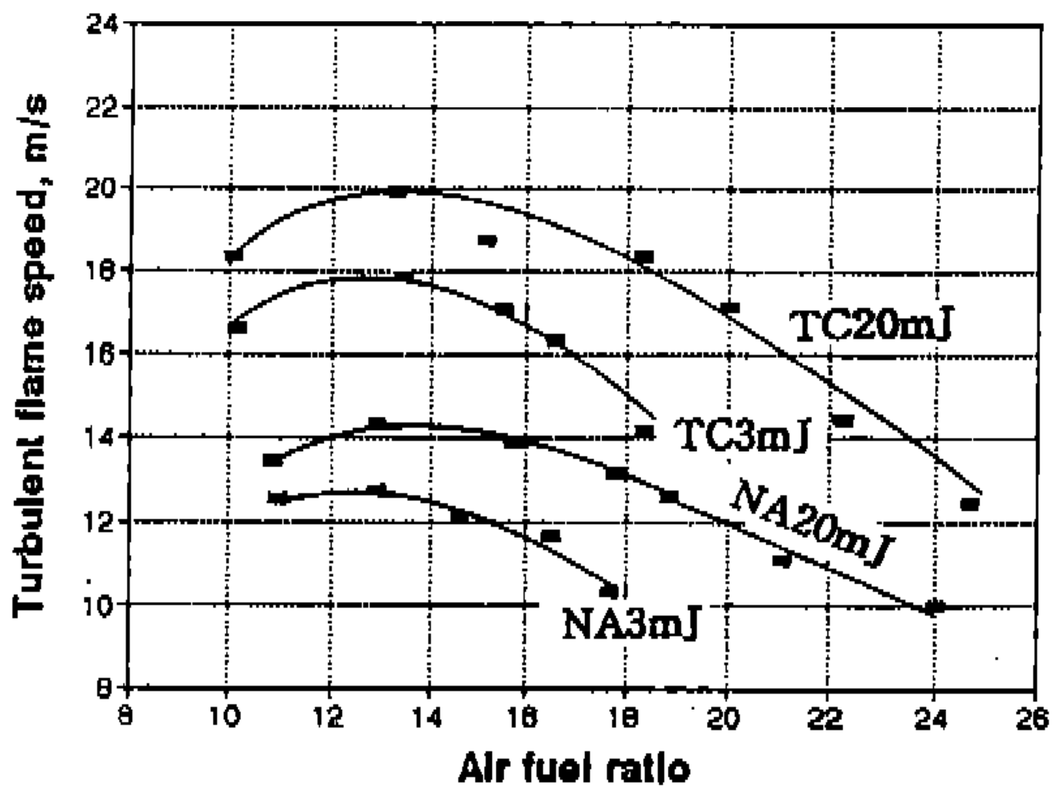

Fig.7 Turbulent flame speed with air fuel ratio

on Richard and Melvin's equation showed the maximum laminar burning velocity 1.7m/s. The maximum laminar burning velocity was 2.5m/s based on Kuehl's equation.

Through the results of Hirano's and the Kuehl's tests, the most appropriate equation of the maximum laminar burning velocity was the Kuehl's equation. EQ(11) shows the laminar burning velocity.

$$V_L = \frac{1.087 \times 10^6}{(10^4/T_f + 900/T_u)^{4.938}} P^{-0.09876}. \quad (11)$$

4.2 Determination of the Minimum Flame Kernel Radius by Lean Misfiring Limit

The proposed EQ(5) of the minimum flame kernel radius gave the theoretical values by using the thermal conductivity, the flame temperature, and the laminar burning velocity. The minimum flame kernel radius was obtained theoretically and was compared to the combustion limit versus the variations of the ignition energies.

Based on EQ(5), the flame kernel radius was calculated during the constant ignition energy supplied. Based on the variation of the ignition energies, the lean burn limits were determined.

The ignition energy E is represneted as follows :

$$E = C_p V \rho_f (T_f - T_u) \quad (12)$$

where the ideal gas state was assumed. Also, the flame kernel radius was calculated.

$$V_L = \sqrt[3]{\frac{3E R T_f}{4\pi C_p P_u (T_f - T_u)}}. \quad (13)$$

The flame kernel radius was obtained by inserting EQ(12) of ignition energy into EQ(13), and was calculated at each ignition energy level.

Finally, the calculated flame kernel radii were compared to the minimum flame kernel radii. Although the minimum flame kernel radii were theoretically calculated, the accuracy of these values were impossible by the ordinary verification methods. The accuracy of the calculated values should be decided by comparing the lean burn limits from the tests with those from the calculations. The ignition device, provided the ignition energies of 3mJ, 14mJ, 20mJ, 24mJ and 28mJ.

Figure 8 shows the flame kernel radius with respect to the variation of the air fuel ratio and the minimum flame kernel radius abtained from the theoretical calculations.

Figure 9 shows the errors of the lean burn limit and the minimum flame kernel radius when ignition energy is increased of. There were two kinds

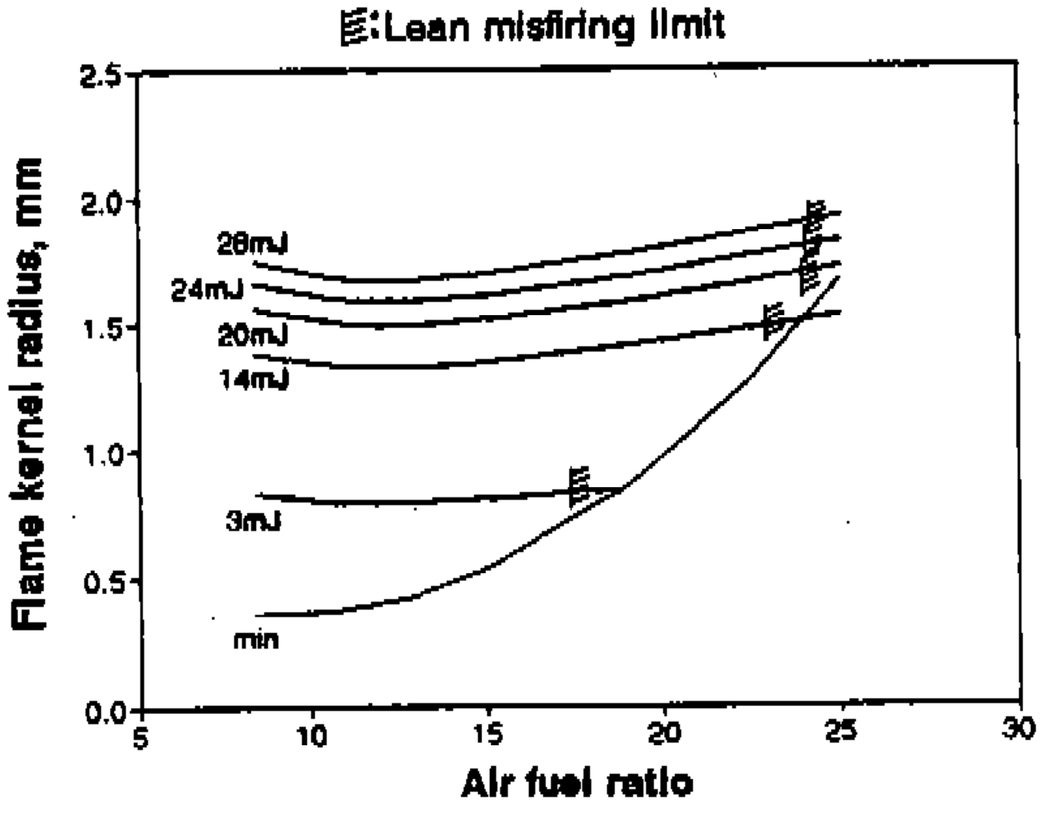

Fig.8 Flame kernel radius with air fuel ratio for discharge energy

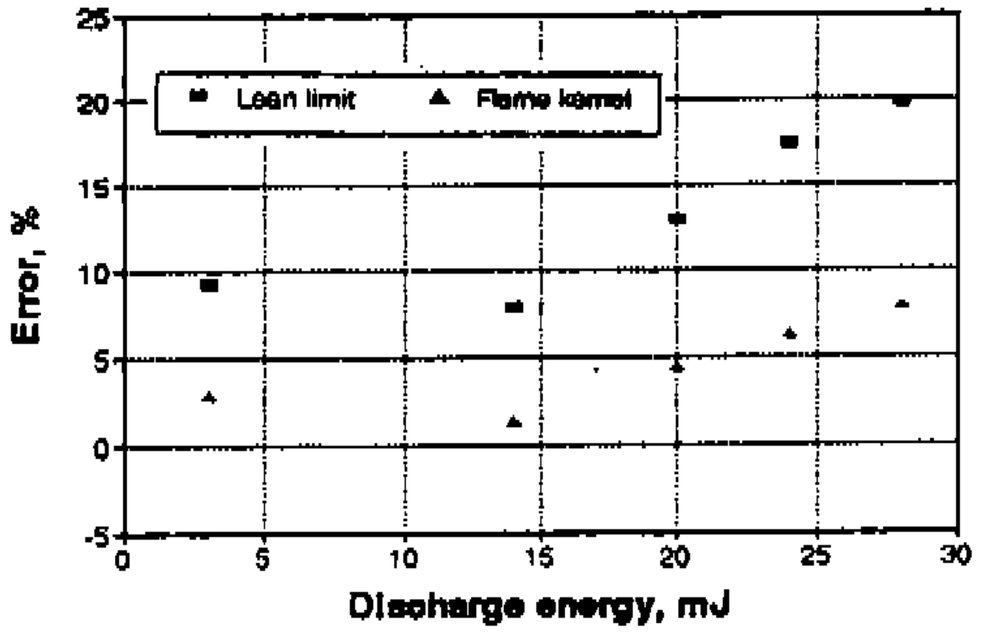

Fig.9 Error of combustion limit and flame kernel with discharge energy

of the lean burn limits to be compared. One was obtained from the operational test and the other was from the theoretical calculation. In the case of 3mJ ignition energy supplied, the theoretical air fuel ratio 17.5 : 1 in the operational test was found. This showed an 8.6 percent error between the theoretical velue and the practical test.

A 2.1 percent error was measured at the 14mJ ignition energy, 5.9 percent error at the 20mJ ignition energy, 9.2 percent error at the 24mJ ignition energy, and 11.7 percent error at the 28mJ ignition energy. All of these were the difference between the theoretical value and the operational test one.

There were also two minimum flame kernel radii defined by the two kinds of the lean burn limits. The one was from the operational test and the other was from the theoretical calculation.

In case of the ignition energy 3mJ supplied, the minimum flame kernel radius calculated was 79.8 μm ; whereas, the minimum flame kernel radius was 78.1μm in the operational test. This showed the 2.2 percent error between each other. The 1.9 percent error was measured at the 14mJ ignition energy, 12 percent error at the 20mJ ignition energy, 2.3 percent error at the 24mJ ignition energy and 3.3 percent error at the 28mJ ignition energy.

The causes of these errors were mainly due to the states of the air fuel mixtures. Although the state of the mixture was actually nonhomogeneous, a homogeneous mixture was assumed in the calculations. Generally, the error between the lean burn limits was 9 percent and the error caused by the minimum flame kernel radii was 2 percent, approximately.

Finally, the minimum flame kernel radii were calculated by taking the deviations from the operational test into account.

5. Conclusions

1) The minimum flame kernel radii based on the theory of thermal ignition were calculated. Previously, the development process of the flame kernel might be obtained by the operational test. The minimum flame kernel radii to avoid misfire were theoretically calculated based on the theory of thermal ignition. Which states that the flame propagates if the heat capacity of the reaction volume is greater than that of the reaction surface.
2) The equation of the minimum flame kernel radius based on the theory of thermal ignitions that the following parameters be known : the thermal conductivity, the flame temperature the laminar burning velocity, and the other thermodynamic properties.
3) To evaluate the accuracy of the minimum flame kernel radius based on the theory, from calculation and those from tests were compared with each other. Also, the minimum flame kernel radii were compared.

References

1. Richard, E. and Patterson, J.D., "Mixture Turbulence—A Key to Cyclic Combustion Variation", SAE Paper 730086, 1973.
2. Harrington, J.A., Shishu, R.C. and Asik, J.R., "A study of ignition system effects on power, emissions, lean misfire limit, and EGR tolerance of a single cylinder engine-multiple spark versus conventional single spark ignition", SAE Paper 740188, 1974.
3. Matsuoka, S., Yamaguchi, T. and Umemura, Y., "Factors Influencing the Cyclic Variations of Combustion of Spark-Ignition Engine", SAE Paper 710586, 1971.
4. Young, M.B., "Cycle Dispersion in the Homogeneous—Charge Spark—Ignition Engine —a Literature Survey", SAE Paper 810020, pp.49-73, 1981.
5. Milkins, E.E., Watson, H.C., Goldsworthy, L.C.

and Hallworth, R.J., "Cycle by Cycle Variability in Emissions of a Spark Ignition Engine", SAE Paper 741034, 1974.

6. Swords, M.D., Alghatgi, G.T. and Watts, A.J., "An Experimental Study of Ignition and Flame Development in a Spark Ignited Engine", SAE Paper 821220, 1982.
7. Boston, P.M., Dradley, D. et al., "Flame Initiation in Lean, Quiescent and Turbulent Mixtures with Various Igniters", Twentieth Symposium (International) on Combustion, the Combustion Institute, pp.141-149, 1984.
8. Quader, A.A., "What Limits Lean Operation in Spark Ignition Engine—Flame Initiation or Propagation", SAE Paper 760760, 1976.
9. Ziegler, G.F.W., Wagner, E.P., Saggau, B., Maly, R. and Herden, W., "Influence of a Breakdown Ignition System on Performance and Emission Characteristics", SAE Paper 840992, 1984.
10. Maly, R., "Ignition Model for Spark Discharges and the Early Phase of Flame Front Growth", 8th Symposium (International) on Combustion, the Combustion Institute, p.1747, 1981.
11. Maly, R. and Ziegler, G., "Thermal Combustion Modeling—Theoretical and Experimental Investigation of the Knocking Process", SAE Paper No.820759, pp.2569-2602, 1982.
12. Sers F.W. and Salinger, G.L., Thermodynamics, Kinetic Theory, and Statistical Thermodynamics, Third Edition, Addison Wesley, pp.276-286, 1976.
13. Van Tiggelen, A. and Deckers, J., "Chain Branching and Flame Propagation", 6th Symposium (International) on Combustion, the Combustion Institute, pp.61-65, 1957.
14. Richard, S.B. and Melvin, G., "Correlation of Burning Velocity, Quenching Distances and Minimum Ignition Energies for Hydrocarbon—Oxygen—Nitrogen System", 6th Symposium (International) on Combustion, the Combustion Institute, pp.66-74, 1956.
15. Kuehl, D.K., "Laminar Burning Velocities of Propane—Air Mixtures", 8th Symposium (International) on Combustion, the Combustion Institute, pp.510-521, 1962.
16. Hirano, M., Oda, K., Hirano, T. and Akita, K., "Burning Velocities of Methanol—Air—Water Gaseous Mixtures", Combustion and Flame, Vol.40, pp.341-343, 1982.